A Simple Millifluidic Benchtop Reactor System for the High-Throughput Synthesis and Functionalization of Gold Nanoparticles with Different Sizes and Shapes

Samuel E. Lohse, Jonathan R. Eller, Sean T. Sivapalan, Michael R. Plews, and Catherine J. Murphy*

Department of Chemistry, University of Illinois at Urbana—Champaign, 600 South Mathews Avenue, Urbana, Illinois 61801, United States

ABSTRACT Despite the continuing interest in the applications of functionalized nanomaterials, the controlled and reproducible synthesis of many important functionalized nanoparticles (NPs) above the milligram scale continues to be a significant challenge. The synthesis of functionalized NPs in automated reactors provides a viable approach to circumvent some of the shortcomings of traditional nanomaterial batch syntheses, providing superior control over reagent addition, improved reproducibility, the opportunity to interface real-time product monitoring, and a viable high-throughput synthetic approach. Here, we demonstrate the construction and operation of a simple millifluidic reactor assembled entirely from commercially available components found in almost any chemical laboratory. This reactor facilitates the aqueous gram-scale synthesis of a variety of functionalized gold nanoparticles, including the synthesis of gold nanospheres with tightly controlled core diameters and gold nanorods with controlled aspect ratios between 1.5 and 4.0. The absolute dimensions (*i.e.*, the transverse diameter) of gold nanorods synthesized within the reactor can also be tailored to produce different gold nanorod shapes, including "small" gold nanorods and gold nanocubes. In addition, we show that the reactor can interface with existing purification and monitoring techniques in order to enable the high-throughput functionalization/purification of gold nanorods and real-time monitoring of gold nanoparticle products for quality control. We anticipate that this millifluidic reactor will provide the blueprint for a versatile and portable approach to the gram-scale synthesis of monodisperse, hydrophilically functionalized metal NPs that can be realized in almost any chemistry research laboratory.

KEYWORDS: gold nanoparticles · flow synthesis · millifluidic reactor · gold nanorod · gram-scale

Despite sustained interest in the optical,[1,2] electronic,[3,4] and theranostic applications[5−13] of functionalized nanomaterials, their controlled and reproducible synthesis, particularly above the milligram scale, remains a challenge.[14−22] Most functionalized nanoparticles (NPs) are still synthesized using discovery phase (low-yield, high-waste, low-throughput) synthetic strategies and purification approaches which are inefficient and generally not amenable to scale up.[13−15,17,22] As nanotechnology enters a more application-oriented phase, however, kilogram-scale quantities of monodisperse NPs will be needed to verify NP performance in biomedical applications, develop prototype devices, and adequately assess their potential toxicity.[13,15−17] For instance, it has been calculated that, in order to supply every person on earth with a 10 nm thick, 2.25 cm^2 monolayer of gold nanoparticles (*e.g.*, as a standardized dose for theranostic anticancer treatments), gold nanoparticles would have to be reliably produced on the 100 kg scale.[17] Currently, even though gold nanoparticle (AuNP) syntheses have been extensively researched for decades, few syntheses produce AuNPs on greater than a 50 mg scale.[14−24] A typical synthesis, the standard seeded-growth synthesis of gold nanorods (AuNRs) produces less than 10 mg of AuNRs per batch.[14,15,18] Though it seems conceptually simple, scaling up gold nanoparticle syntheses is a significant challenge. Increasing the concentration of the reagents in the growth solution, or even the volume of the reaction can significantly alter the rates reagent diffusion and thermal transport,

* Address correspondence to murphycj@illinois.edu.

Received for review January 30, 2013 and accepted May 1, 2013.

Published online May 01, 2013
10.1021/nn4005022

effectively resulting in a loss of control over product properties.[16,22,25] Accordingly, in order to meet the demand for adequate nanomaterial testing and prototype development, new strategies and infrastructure for nanomaterial synthesis must be implemented.[25]

The silver-assisted seeded growth synthesis of low aspect ratio AuNRs provides a convenient example of the advantages and drawbacks of the typical discovery phase NP synthesis.[15,18] This synthesis involves the addition of a small gold nanoparticle seed to a growth solution containing cetyl trimethyl ammonium bromide (CTAB), hydrogen tetrachloroaurate, silver nitrate, and ascorbic acid, facilitating the slow anisotropic growth of single-crystalline AuNRs.[1,15,18] Although this synthesis provides exceptional control over nanoparticle shape, readily yielding AuNRs with precisely controlled aspect ratios between 1.5 and 4.0, only approximately 15% of the initial gold is converted to gold nanorods (~7 mg AuNR/100.0 mL reaction solution).[15,16,18] Compared to many functionalized NP syntheses, this synthesis is relatively scalable, as gold nanorods prepared by this method are commercially available in appreciable quantities from several retailers in concentrations of >30 ppm (Sigma-Aldrich, Nanopartz, Nanoseedz, *etc.*). However, in the typical research laboratory, it still remains challenging to produce these AuNRs on anything near the gram scale.

Recent modifications to the silver-assisted synthesis of AuNRs have provided a means to improve product monodispersity and extended the range of AuNR aspect ratios that can be synthesized using this approach;[24] however, attempts to translate this general approach to a gram-scale synthesis for AuNRs have met with limited success.[22,23] Jana demonstrated a gram-scale synthesis for AuNRs in 2005 (which uses sodium borohydride, rather than spherical AuNP seeds as a reaction initiator), but this gram-scale synthesis primarily produces AuNRs with very small transverse diameters (~6.0 nm).[22] In addition, this synthesis requires significant increases in the concentration of the reagents in the nanorod growth solution, which in turn induces the formation of an insoluble Au−Br−CTA complex. This reduces the homogeneity of the reaction mixture, and leads to increased polydispersity in the products at the gram scale.[22] Zubarev recently developed an alternative synthesis that requires the slow, mediated addition of an excess of ascorbic acid to produce a very monodisperse AuNR product (σ ~3%) at the gram scale.[23] However, the increased ascorbic acid required in the synthesis favors the formation of gold nanorods with large transverse diameters (~25.0 nm), meaning that the overall synthetic control over gold nanorod dimensions provided by this approach is again somewhat limited.[23] As these examples show, while altering NP synthesis conditions to achieve gram-scale synthesis can be effective in producing a gram of material, there is often a corresponding trade-off in the ability to control the dimensions of the product NPs.

An alternative approach to improving the quality and throughput of functionalized NP synthesis involves transferring their synthesis from familiar batch reactors (*e.g.*, round-bottomed or Erlenmeyer flasks) to automated reactors (particularly microfluidic devices).[25] Automated synthesis reactors include microfluidic devices,[25−38] millifluidic reactors,[39−42] and even dedicated robotic workstations.[43] These automated reactors are an appealing option for the high-throughput synthesis of monodisperse functionalized nanomaterials because they theoretically allow researchers to achieve gram-scale synthesis by continuous operation of the reactor, or "numbering up" and running multiple reactors in parallel, thus avoiding the typical challenges associated with scaling up a synthesis in batch.[25] In addition, their narrow reaction channels and customized mixing geometries can provide very precise control over the timing of reagent addition and improved thermal transport properties, two factors that strongly influence the monodispersity of the product nanomaterials.[25−43] Moreover, synthesis in automated reactors provides an opportunity to directly interface analytical techniques (such as UV−vis absorbance or emission spectroscopy) with nanomaterial synthesis, enabling new options for online monitoring and real-time quality control.[25,37,38] As a result, product quality in flow synthesis can be controlled independently of reaction scale, and synthesis in fluidic reactors potentially provides the opportunity to monitor the quality of the product while the synthesis progresses, further improving property control and reducing wasted material.

Over the last five years, a number of researchers have recognized the potential benefits of functionalized nanoparticle synthesis in automated reactors (particularly microfluidic devices), and have shown that these reactors can be used as synthesis environments for the preparation of various semiconductor and metal nanoparticles.[25] In several instances, NP populations with improved quality (in terms of the core diameter polydispersity) have resulted from transferring the synthesis to a flow environment.[25] However, many challenges remain in optimizing the automated synthesis of functionalized colloidal nanoparticles: reliable strategies for NP size control during synthesis in reactors have not yet been fully established, the synthesis of more complex nanoparticles (*e.g.*, anisotropic shapes or core:shell structures) has not been extensively investigated, and characterization of the final products has been somewhat limited.[25] In addition, no one has yet demonstrated that the theoretically improved throughput of the automated synthesis of nanomaterials can be translated to the production of increased yields of material either through the continuous operation of a single reactor or numbering up separate microfluidic devices.

Each type of automated reactor platform has different advantages and disadvantages for the synthesis of functionalized nanoparticles.[25,37−43] Microfluidic devices, though they can provide exquisite control over the timing of reagent addition and new strategies to control mixing, have proven to be highly susceptible to irreversible fouling (blockage) during nanoparticle synthesis and numbering up the reactors to provide gram-scale synthesis has proven to be challenging.[25,37−39] In addition, microfluidic reactors are expensive and time-consuming to fabricate, and therefore, any reactor fouling which occurs during synthesis results in long delays while new devices are fabricated.[25,39,40] Dedicated robotic workstations can be constructed which provide even greater control over reagent addition and ambient conditions than microfluidic devices.[43] These workstations can interface with highly sophisticated monitoring/characterization techniques making them ideal for high-throughput method design and highly reproducible NP synthesis. Unfortunately, only a handful of such workstations exist, and are housed in shared user facilities.[43] An alternative to synthesis in microfluidic devices, or sophisticated robotic workstations, is the synthesis of colloidal functionalized NPs in millifluidic reactors (reactors that possess channels with mm dimensions).[39,40] Millifluidic reactors provide many of the same advantages during synthesis as microfluidic devices, yet are easier to fabricate, better resist fouling, and are easier to interface with typical laboratory instrumentation for quality control.[39−42] As a result, millifluidic reactors are ideally positioned to serve the needs of academic research laboratories that require a simple and robust system to facilitate the scale-up of NP syntheses without compromising size or shape control. Despite the potential facility of millifluidic reactors for nanomaterials synthesis, however, these systems have received little formal research attention.[39−42]

Herein, we demonstrate the construction and operation of a simple millifluidic flow reactor that enables the controlled high-throughput synthesis of a variety of functionalized AuNPs, easily extending their syntheses up to the gram scale, while integrating real-time quality control and purification. Our initial demonstration of the reactor focuses on various room temperature syntheses of ligand-stabilized gold nanoparticles, including the synthesis of CTAB-stabilized spheres, ω-functionalized thiol-stabilized spheres, citrate-stabilized spheres, and CTAB-stabilized gold nanorods while maintaining excellent control over nanoparticle size and aspect ratio. The AuNPs synthesized within the reactor show slightly superior monodispersity *versus* the corresponding batch syntheses, even though the reactor permits synthesis of gold nanoparticles at higher concentrations than are typically achieved in batch. Synthesis in the flow reactor also provides an opportunity to precisely manipulate the dimensions of gold nanorods during synthesis including overgrowth of AuNRs or the synthesis of `small' AuNRs. Crucially, the use of the millifluidic reactor easily extends AuNP synthesis up to the gram scale, as a gram of gold nanorods with precisely controllable aspect ratios can be prepared in less than four hours of reactor operation. By integrating a commercially available flow-through cuvette into the reactor line, the quality of the products can be monitored in real-time using UV−vis absorbance spectroscopy. Finally, the use of the peristaltic pump to drive the flow reactor also provides an opportunity to interface the reactor with commercially available purification technology, facilitating high-throughput AuNP functionalization. We believe this versatile millifluidic flow reactor (which can be assembled and operated in almost any chemistry laboratory) can serve as a model integrated production platform for hydrophilically functionalized monodisperse gold nanoparticles convenient for a variety of laboratory settings.

RESULTS AND DISCUSSION

Our millifluidic reactor is assembled entirely from commercially available components that can be found in most any laboratory, and effectively facilitates high-throughput gold nanoparticle synthesis, purification/functionalization, with integrated real-time analysis (Figure 1). The reactor is driven by the peristaltic pump which can drive fluid flow through the system at flow rates between 1.0 and 100.0 mL/min. We find that pump operation at flow rates between 35.0 and 60.0 mL/min generally provides the synthesis of the most mondisperse gold nanoparticles (Supporting Information, Figure S1). The millifluidic flow reactor is assembled from commercially available TYGON poly vinyl tubing, polyethylene mixers, and joints. Mixing of solutions within the reactor was driven by the peristaltic pump (Figure 1a). Gold nanoparticle synthesis in the reactor is initiated through the mixing of two solutions: a growth solution and a reaction initiator solution (containing either a reducing agent [*e.g.*, sodium borohydride] or gold nanoparticle seeds). The two reagent streams are mixed in the Y-mixer primarily by diffusion; calculation of the Reynolds number for the reactor's mixing geometry indicates that fluid flow is primarily in the laminar regime (Figure 1b, Supporting Information).[40,41] Following the initiation of the growth reaction at the Y-mixer, the reaction mixture remains in the reactor for a set residence time, which was simply controlled by varying the length of tubing between the mixer and collection flask (Figure 1a). During our synthesis experiments, residence time was varied between 3.0 and 25.0 min. The majority of direct synthesis in the millifluidic reactor were run at a 3 min residence time. Seeded growth reactions generally experienced a residence time of 20 min. After exiting

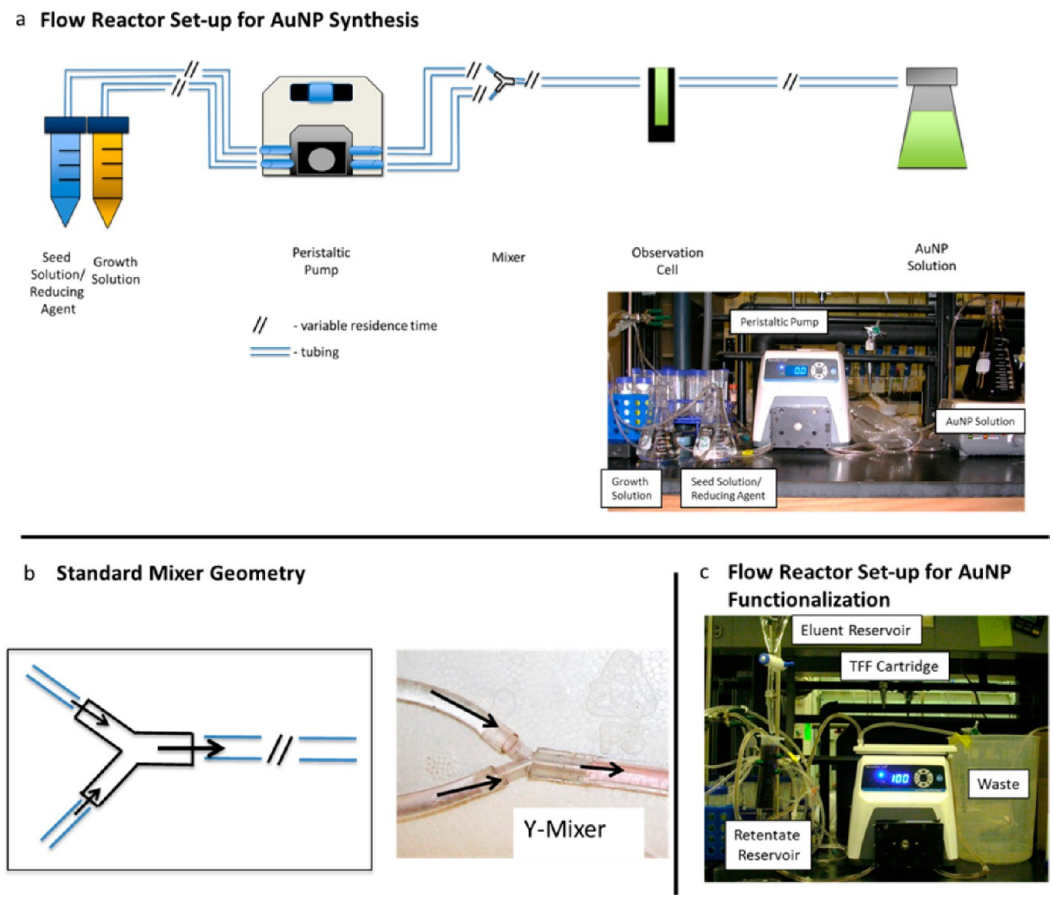

Figure 1. The integrated millifluidic reactor used for gold nanoparticle synthesis and functionalization is shown. (a) Diagram and picture of the reactor for AuNP synthesis. The reactor is composed of multiple modular commercially available components, and fluid flow is driven by the peristaltic pump. (b) In this reactor, mixing of the growth solution and the seed/borohydride solution occurs in a simple polyethylene Y-mixer. (c) The reactor also features an integrated flow-based purification system, in which a commercially available tangential flow filtration cartridge can be attached to an additional peristaltic pump for an integrated high-throughput approach for nanoparticle purification or functionalization.[44]

the reactor, the gold nanoparticle solutions were collected and stirred in an aqua regia-cleaned Erlenmeyer flask, prior to purification. The reactor can be integrated with real-time UV−vis absorbance spectroscopy analysis to enable product monitoring during synthesis, simply by incorporating a flow-through observation cell at variable residence times (Figure 1a) and the reactor can also be integrated with existing flow-based NP purification techniques (*e.g.*, diafiltration, Figure 1c).[44]

During the course of our studies, we sought to illustrate four basic attributes of the millifluidic reactor. (I) The reactor is versatile; in its basic configuration, it can provide an effective high-throughput synthetic platform for a variety of different hydrophilic functionalized gold nanoparticles. (II) The operation of a single reactor facilitates the efficient synthesis of functionalized AuNPs on the gram scale, while maintaining precise control over AuNP size and shape. (III) The reactor easily interfaces with typical laboratory optical spectroscopy instrumentation to provide facile real-time quality control. (IV) The reactor can be interfaced with commercially available high-throughput purification techniques to enable rapid AuNP purification and functionalization. This combination of attributes makes the millifluidic reactor described here a versatile (and potentially portable) platform for the production of hydrophilic functionalized NPs that can be operated in almost any laboratory

Synthesis of Gold Nanoparticles with Controlled Size, Shape, and Surface Chemistry in the Millifluidic Reactor. While a variety of functionalized NPs have previously been synthesized in automated reactors,[25−43] the synthesis of AuNPs with precisely controlled sizes and shapes in a flow environment remains a pertinent research challenge.[25] We set out to demonstrate that our millifluidic reactor was a versatile platform suitable for the synthesis of a number of different types of functionalized AuNPs with precisely controlled sizes and shapes. We therefore attempted to synthesize a wide library of functionalized AuNPs in the millifluidic reactor, including spherical AuNPs with precisely controlled sizes and different surface chemistries, as well as gold nanorods with different aspect ratios and absolute dimensions (Figure 2).[16,18−23,44−53] Consequently, we synthesized a library of functionalized AuNPs with controlled core size, shape, and surface chemistry, including: citrate

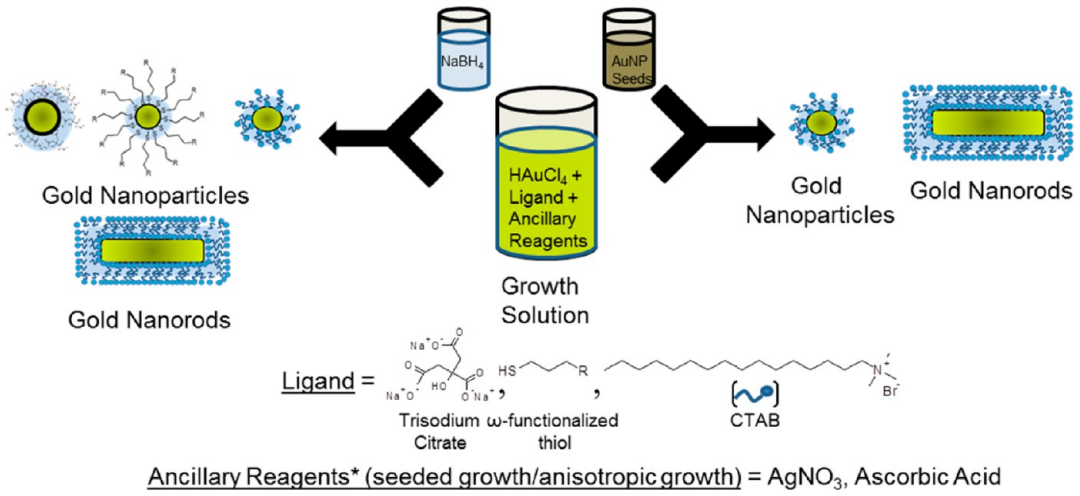

Figure 2. Diagram of the AuNP synthetic strategies employed in the millifluidic reactor. Gold nanoparticles were synthesized either by the addition of sodium borohydride (direct synthesis) or small gold nanoparticle seeds to growth solutions containing combinations of gold tetrachloroaurate, capping agents (trisodium citrate, functionalized thiols, CTAB), and ancillary reagents ($AgNO_3$, ascorbic acid [if necessary]). Various sizes and shapes of AuNPs including spherical and rod-shaped AuNPs can be successfully prepared using this approach.

(Cit)-stabilized, mercaptohexanoic acid (MHA)-stabilized, and CTAB-stabilized spherical AuNPs, and CTAB-stabilized gold nanorods (AuNRs) within the millifluidic reactor. Cit-AuNPs, MHA-AuNPs, and small CTAB-AuNPs (d_{core} < 10.0 nm) were prepared by direct reduction with sodium borohydride.[16,46,47,49] Larger CTAB-AuNPs and CTAB-stabilized AuNRs were prepared using seed-mediated growth techniques.[16,45,48] Within the reactor, the size and dimension of all particles were controlled using the same synthetic parameters as in the corresponding batch syntheses (Ligand:Au ratio, $AgNO_3$ concentration, *etc.*).[1,16]

We first attempted to prepare a variety of CTAB-stabilized AuNPs with core diameters between 2.0 and 40.0 nm (specifically 2.0, 8.0, 20.0, and 40.0 nm cores) using a combination of direct reduction and seeded growth approaches.[45] Direct borohydride reduction was used to synthesize CTAB-stabilized gold nanoparticles with core diameters less than 8.0 nm.[16,45] In these syntheses, the millifluidic reactor was run at a flow rate of 50.0 mL/min, and the reaction solution was held in the reactor for a residence time of 3.0 min, before being deposited in the collection flask. By varying the BH_4:Au ratio used in the direct reduction, we were able to synthesize CTAB-AuNPs with core diameters of 2.0 ± 0.4 nm (N = 453) and 8.2 ± 2.0 nm (N = 745), as determined by TEM (Figure 3 I and ii, Table 1). Larger CTAB-AuNPs were prepared by using the 8.0 nm CTAB-AuNPs as seeds in a standard seeded growth procedure.[45] This produces CTAB-AuNPs with a core diameter of 20.7 ± 4.5 nm (N = 402). These can, in turn, be used as seeds in the synthesis of 40.0 nm CTAB AuNPs (37.0 ± 2.7 nm, N = 150). The synthesis of CTAB-AuNPs with controlled sizes over such a wide range of core diameters shows that the millifluidic reactor that we have assembled can be used to prepare a wide range of AuNP sizes, yet maintain tight control over the core diameter dispersity.

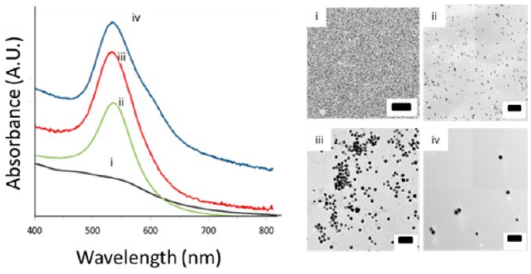

Figure 3. CTAB-stabilized spherical AuNP with precisely controlled sizes prepared in the millifluidic flow reactor. UV−vis absorbance spectra TEM images of 2.0 nm (i), 8.0 nm (ii), 20.0 nm (iii), and 40.0 nm (iv) CTAB-stabilized gold nanoparticles are shown. Spectra are offset for clarity. Size analysis of the TEM images reveals the core diameter of these AuNPs to be: (i) 2.0 ± 0.4 nm, N = 453 (scale bar is 20 nm); (ii) 8.2 ± 2.0 nm, N = 745 (scale bar is 50 nm); (iii) 20.7 ± 4.5 nm, N = 402 (scale bar is 50 nm); (iv) 37.0 ± 2.7 nm, N = 150 (scale bar is 200 nm).

In addition, small Cit-AuNPs (d_{core} ~4.0 nm) and MHA-AuNPs (d_{core} ~2.0 nm) were synthesized in the millifluidic reactor by direct reduction with sodium borohydride.[16,20,44,46,47] The citrate-stabilized AuNP solution was red-orange in color, possessing a weak surface plasmon resonance absorption maximum (λ_{max}) of 517 nm (Table 1). TEM analysis indicated a core diameter of 4.1 ± 1.1 nm (N = 1295, Supporting Information) for the Cit-AuNPs. The MHA-AuNP solution was a deep brown color with an extremely weak plasmon absorbance indicating the formation of AuNPs with a core diameter less than 3.0 nm. TEM analysis of these particles gave the core diameter as 2.2 ± 0.5 nm (N = 989, Supporting Information).[56] The millifluidic reactor can therefore be used to prepare a variety of gold nanoparticles with different surface chemistries.

TABLE 1. Spherical Gold Nanoparticles Synthesized in the Flow Reactor

AuNP sample	ligand	core diameter (nm)	SPR λ_{max} (nm)	estimated throughput (mg/min)[a]
2.0 nm CTAB-AuNPs	CTAB	2.0 ± 0.4	[b]	[b]
8.0 nm CTAB-AuNPs	CTAB	8.2 ± 2.0	518	1.20 ± 0.10
20.0 nm CTAB-AuNPs	CTAB	20.7 ± 4.5	532	0.57 ± 0.06
40.0 nm CTAB-AuNPs	CTAB	37.0 ± 2.7	539	0.74 ± 0.04
2.0 nm MHA-AuNPs	Mercaptohexanoic acid	2.2 ± 0.5	[b]	[b]
4.0 nm Cit-AuNPs	Citrate	4.1 ± 1.1	517	0.37 ± 0.05

[a] Throughput calculation based on AuNP concentration determined from UV–vis data.[54] [b] AuNPs too small to determine accurate concentration from UV–vis.

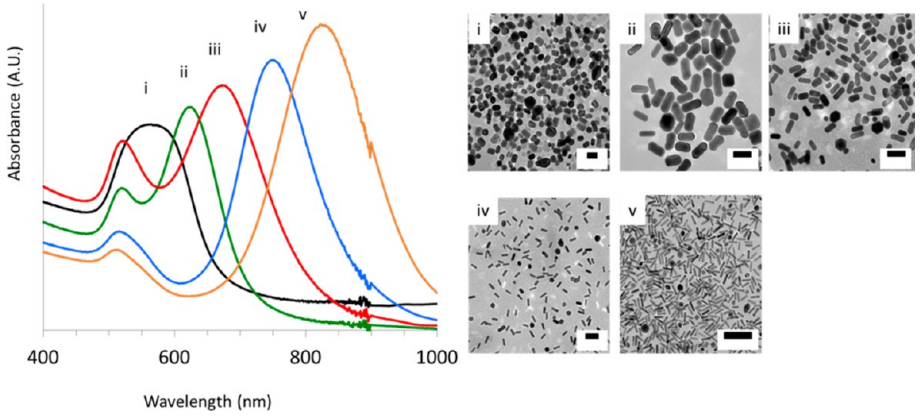

Figure 4. Gold nanorods of varying aspect ratio can be prepared within the flow reactor using a seeded growth approach. UV–vis absorbance spectra and TEM images of five different AuNR aspect ratios. The aspect ratio of the gold nanorods can be tuned between 1.5 and 4.0. (i) AuNRs AR = 1.5. (ii) AuNRs AR = 2.0. (iii) AuNRs AR = 2.5. (iv) AuNRs AR = 3.0. (v) AuNRs AR = 3.5. Scale bars are 50 nm.

TABLE 2. Gold Nanorods Synthesized in the Flow Reactor

AuNR sample	dimensions (nm)	SPR λ_{max} (nm)	estimated throughput (mg/min)[a]
AuNR AR = 1.5	49.2 ± 6.3 × 34.2 ± 4.8	556	0.58 ± 0.07
AuNR AR = 2.0	47.4 ± 5.7 × 24.7 ± 4.9	508, 640	0.43 ± 0.02
AuNR AR = 2.5	39.2 ± 6.4 × 17.5 ± 2.2	512, 690	0.54 ± 0.05
AuNR AR = 3.0	31.0 ± 5.8 × 12.1 ± 1.2	511, 787	0.25 ± 0.03
AuNR AR = 3.5	27.8 ± 5.4 × 7.5 ± 1.4	509, 824	0.41 ± 0.04
"small" AuNR AR = 2.0	13.5 ± 2.2 × 6.6 ± 1.0	509, 698	[b]
"small" AuNR AR = 3.0	16.5 ± 3.6 × 6.1 ± 1.2	512, 795	[b]

[a] Throughput calculation based on AuNP concentration determined from UV–vis data.[18] [b] [AuNR] could not be determined via UV–vis as the extinction coefficients for the small AuNRs have not been fully determined.

We further extended the synthesis of AuNPs in our millifluidic reactor to the synthesis of gold nanorods with controlled aspect ratios.[18,48] To prepare gold nanorods, small CTAB-stabilized gold seeds (2.0 nm in diameter) were mixed in the reactor with a growth solution containing gold tetrachloroaurate, CTAB, silver nitrate, and ascorbic acid.[18,48] This resulted, as expected, in the formation of CTAB-stabilized gold nanorods with different aspect ratios between 1.5 and 4.0, as determined by UV–vis absorption analysis and TEM. It is well-known that the silver ion concentration in the growth solution controls the aspect ratio of these resulting rods.[18,48] The gold nanorods produced by this method had a transverse diameter of approximately 12.0 nm and lengths ranging from 28.0 to 50.0 nm (Figure 4, Table 2), consistent with the established upper and lower aspect ratio values for AuNRs synthesized using this seeded growth approach.

Controlling the Absolute Dimensions of Gold Nanorods within the Capillary Flow Reactor. We attempted to demonstrate that not only could the aspect ratio and size of AuNRs and AuNPs be controlled during synthesis in the millifluidic reactor, but also that the shape and absolute dimensions of the AuNRs could be similarly controlled. We therefore adapted two reported syntheses of gold nanorods of irregular shape or size and applied them to millifluidic flow environment.[49–53] These syntheses included the "overgrowth" of AuNRs to yield "fat"[51–53] AuNRs and the synthesis of "small" AuNRs.[49,50]

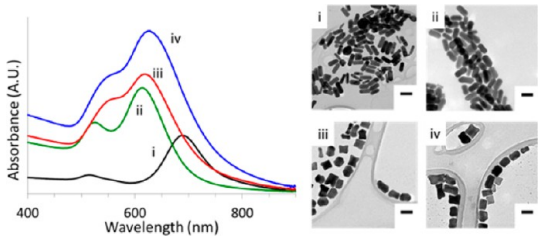

Figure 5. The shape of the gold nanorods can easily be fine-tuned in the reactor through overgrowth. UV−vis spectra and TEM images of four AuNR shapes are shown. (i) Gold nanorods prepared using the standard ascorbic acid concentration. Au:Asc *A* = 1:1 (molar ratio). (ii) Increasing the ascorbic acid leads to `fatter' gold nanorods; the result of isotropic overgrowth around the gold nanorods. Au:Asc *A* = 1:1.4. (iii) Further ascorbic acid leads to the formation of dog-boned gold nanorods. Au:Asc *A* = 1.7. (iv) Finally, gold nanorods become enlongated cubes at the highest ascorbic acid concentration. Au:Asc *A* = 2.0. Scale bars are 100 nm.

The overgrowth of AuNRs to yield AuNRs with large transverse diameters ("fat" AuNRs) can be performed by increasing the ascorbic acid concentration used in the seeded growth synthesis.[51−53] The increased ascorbic acid concentration leads to additional isotropic overgrowth following the initial anisotropic growth phase of nanorod formation. Accordingly, we increased the ascorbic acid concentration in our seeded growth synthesis from 1.1 to 2.0 mols ascorbic acid: mols Au(III). We found that increasing the ascorbic acid to gold ratio indeed provided an opportunity to "coarsen" the rods, leading to increased transverse diameters. Significant morphological changes in the rods were observed for every additional 0.3 mol equiv of ascorbic acid added. The UV−vis absorbance spectra and TEM images of these AuNRs are provided in Figure 5. After the addition of 1.4 mol equiv of ascorbic acid, the rods maintained the same length (49.1 ± 5.8 nm for Figure 5i *versus* 47.1 ± 7.8 nm for Figure 5ii), but fattened slightly, resulting in an aspect ratio decrease from 2.6 ± 0.3 (Figure 5i) to 2.1 ± 0.2 (Figure 5ii) [*N* = 50]. The coarsening of the AuNRs was reflected in the blue shift in the longitudinal plasmon maxima from 690 to 620 nm in the UV−vis spectrum. The addition of 1.7 mol equiv of ascorbic acid to the reaction mixture caused a further fattening of the gold nanorods to produce dog-boned gold nanorods structures (Figure 5iii). Addition of 2.0 mol equiv of ascorbic acid to the reaction mixture produced gold nanocubes (Figure 5iv).

We also demonstrated the synthesis of "small" AuNRs (AuNRs with small transverse diameters) in the millifluidic reactor.[22,49,50] The synthesis of "small" AuNRs is accomplished by a direct reduction of a typical AuNR growth solution by sodium borohydride. The transverse diameter of these "small" nanorods are only 4−10 nm, yet the aspect ratio-dependent optical properties of these AuNRs are quite similar to the optical properties of the more common single-crystalline AuNRs with aspect ratios between 1.5 and 4.0, as has previously been observed.[49]

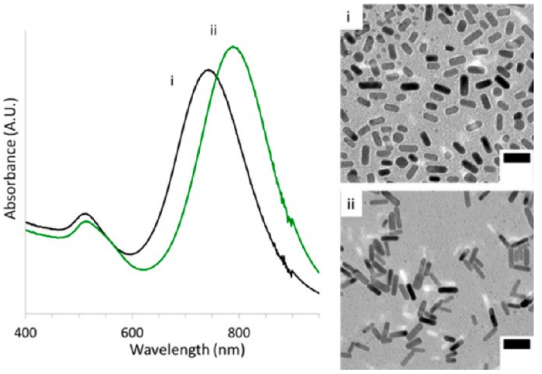

Figure 6. UV−vis absorbance spectra and TEM images for the solutions of small gold nanorods with different aspect ratios prepared in the millifluidic reactor. (i) Small gold nanorods with aspect ratio ~2.0. (ii) Small gold nanorods with aspect ratio ~3.0. Scale bars are 25 nm.

In our case, rods produced by borohydride reduction had a transverse diameter of approximately 7 nm, and a longitudinal diameter of between 12 and 17 nm. Consistent with what has previously been reported by Jana and, more recently, by Ali, the aspect ratio of these "small" gold nanorods could be controlled by varying the concentration of sodium borohydride used in the synthesis (Figure 6).[22,50] By decreasing the borohydride concentration used in the synthesis from 1.5 to 0.05 mM, the aspect ratios of the rods were increased from 2.0 (LSPR = 700 nm) to 3.0 (LSPR = 795 nm). The aspect ratio 2 AuNRs have a transverse diameter of 6.6 ± 1.0 nm and a length of 13.5 ± 2.2 nm, giving an average aspect ratio of 2.0 ± 0.1 (*N* = 100). The aspect ratio 3 AuNRs have a transverse diameter of 6.1 ± 1.2 nm and a length of 16.5 ± 3.8 nm, giving an average aspect ratio of 2.8 ± 0.5 (*N* = 100).

Characterization of AuNP Surface Chemistry. Functionalized gold nanoparticles prepared in the flow reactor were analyzed by FTIR, TGA, XPS, and ζ-potential analysis to investigate the surface chemistry of the purified AuNPs. Prior to analysis, the AuNPs were purified by either centrifugation or extensive diafiltration (40 volume equiv) to remove excess ligands and possible small AuNP byproducts.[44] ζ-Potential analysis of the purified AuNP samples indicated that the AuNPs show the expected surface charges (Supporting Information, Table S1). MHA AuNPs showed a highly negative ζ-potential, while citrate AuNPs have only moderately negative ζ-potential values. All the CTAB-stabilized AuNPs show the expected positive ζ-potential values.

The presence of the expected functional groups in the ligand shells on the AuNP surfaces is further indicated by FTIR analysis of the purified AuNPs (Supporting Information, Figure S9, S10).[16,18,22,46−50] In addition, XPS analysis indicates that the AuNPs prepared in the millifluidic reactor have a surface composition which is similar to the corresponding AuNPs prepared in batch. CTAB-stabilized AuNPs show

peaks for gold, bromine, carbon, and nitrogen. CTAB-stabilized gold nanorods show the same peaks, but also show a peak for silver, which is consistent with the presence of silver near the AuNR surface, as has previously been observed.[18] No significant differences in composition were noted for the "small" AuNRs (prepared vis borohydride reduction) *versus* the "regular" single-crystalline AuNRs (prepared by seeded growth). XPS analysis of the MHA-stabilized AuNPs show the expected peaks for gold, carbon, and thiolate sulfur, indicating successful formation of the thiolate ligand shell on the AuNP surface.[46,47]

On the basis of the compositional analysis of the AuNP surfaces, it can be seen that functionalized AuNPs prepared in the millifluidic environment have comparable stability to AuNPs prepared by the analogous batch techniques.[16,18,22,23,46,47] Therefore, we expect that synthesis in the millifluidic environment preserves both AuNP size control during synthesis, and ligand shell quality (providing AuNPs of identical quality to cutting edge batch synthesis techniques), while facilitating superior throughput and control over the timing of reagent addition.

Comparison of AuNP Synthesis in the Millifluidic Reactor to Previous Batch and Microfluidic Reactor Syntheses. The spherical gold nanoparticles prepared using the millifluidic reactor possess a comparable core diameter dispersity compared to AuNP products synthesized using established batch techniques. For instance, the CTAB-stabilized AuNPs prepared in our reactor have a dispersity (1σ) of 10−20%, which is essentially identical to the dispersity reported for the original batch synthesis approach.[16,18,48] The core diameter dispersity of the AuNP products prepared in the millifluidic reactor also compares favorably to AuNPs synthesized in microfluidic devices, which are also typically between 10 and 25% of the mean core diameter.[25−38] For the direct synthesis of spherical AuNPs performed in the millifluidic reactor, the yield of AuNPs (percent conversion of starting gold salt to AuNPs, as determined by UV−vis) is essentially identical to the percent yield in the batch synthesis (∼95% of the gold precursor is converted to AuNPs).[16,47,54]

With respect to synthesis by seeded growth (particularly the synthesis of gold nanorods), the millifluidic reactor provides the same degree of control over AuNR shape as the corresponding batch techniques, yet provides some additional advantages, including a modest improvement in yield, and the ability to easily scale the reaction up. In the millifluidic reactor, AuNRs with aspect ratios between 1.5 and 4.0 (LSPR λ_{max} 600−900) can easily be synthesized. This corresponds exactly to the range of low aspect AuNRs that can be synthesized using this approach in batch (although very recent modifications to the silver-assisted synthesis have now extended the upper limit of this synthesis to ∼1400 nm).[18,24,48] The AuNRs synthesized in the millifluidic reactor occur in greater than 95% relative to the total number of particles, with the other 5% being spheroids. This again is identical to the relative ratio of rods:spheres which occur in the silver-assisted seeded growth batch synthesis.[48] However, the silver-assisted seeded growth synthesis in the millifluidic reactor does facilitate the synthesis of AuNRs in slightly higher yield than is typical in the batch synthesis: 22.6 ± 1.1% conversion of gold salt to AuNRs in the millifluidic synthesis relative to 14.7 ± 0.6% in the batch synthesis.[18] Furthermore, the millifluidic reactor permits the synthesis of AuNPs at higher concentrations than are typically achieved in batch by allowing users to scale up the starting reagent concentrations 5−10x and still retain tight control over the product AuNP size and shape. For instance, we found that gold nanorods could be synthesized at up to 3.0 nM in particles, which is ∼5× the concentration of AuNRs synthesized using the analogous silver-assisted seeded growth batch technique.[18,48] Increasing the reagent concentration in the corresponding batch seeded growth synthesis did not result in a corresponding increase in the product concentration (Supporting Information, Figure S6). This means that the millifluidic reactor extends AuNR throughput up to ∼5× the values given in Table 2 (which are the throughput values for the silver-assisted seeded growth synthesis in the reactor at standard concentrations).[18] This gives a maximum throughput of up to 2.5 mg/min, suggesting that gram-scale synthesis of any functionalized gold nanoparticle can be achieved simply by continuous running of the flow reactor (Tables 1 and 2). We believe that the synthesis of monodisperse AuNPs at high concentrations is facilitated by the mixing of relatively small volume elements in the reactor mixer which permits continuous synthesis at high concentrations while simultaneously providing precise control over AuNP dimensions.[25−41] The synthesis of AuNPs at higher concentrations than can be achieved in batch has recently been reported in at least one other millifluidic reactor.[41] Therefore, we deem that synthesis in the millifluidic reactor provides no inherent improvement in AuNP size control or dispersity *versus* the corresponding batch syntheses, but instead provides opportunities to facilitate large-scale syntheses of these AuNPs by providing modest improvements in yield and the ability to synthesize AuNPs at higher concentrations than can be achieved in batch without sacrificing the requisite control over AuNP properties provided by the original synthesis.

The millifluidic reactor that we describe here is designed to function as a high-throughput synthesis device best suited for use in an individual research laboratory. The fact that the reactor can be assembled from commercially available components (and that the basic reactor setup permits the high-throughput

synthesis of many different types of gold nanoparticles) makes the reactor more convenient for high-throughput AuNP synthesis in most research laboratories than microfluidic devices.[25,41] The synthesis of AuNPs (both spherical and anisotropic) in microfluidic devices has been reported several times previously, and a variety of AuNPs including citrate, CTAB, polyvinylpyrrolidone (PVP), and thiol-stabilized spherical AuNPs, as well as AuNRs have been prepared in these devices.[25−27,31,38,41] At least one report of small AuNP synthesis in a millifluidic device has also recently been released.[40] While a variety of AuNPs have been prepared in these microfluidic devices, the ability to effectively control AuNR shape (specifically aspect ratio),[26,29,34] has been shown to be somewhat limited, and contamination of the AuNR samples with excess spherical AuNPs is common.[26,29,34] Furthermore, the microfluidic devices are often susceptible to fouling within hours of operation, which necessitates the fabrication of an entirely new device each time.[25,39,40] Our millifluidic reactor shows no propensity for fouling, as it is capable of operation for greater than 5 h (10 L or more of solution) without any fouling observed, or significant changes in the product properties (Supporting Information, Figure S1). As a consequence, we projected that gram-scale synthesis of AuNPs could be relatively easily achieved simply by continuous operation of the millifluidic reactor.

Gram-Scale AuNR Synthesis in the Millifluidic Reactor. Although microfluidic devices (and other flow reactors) can, in theory, be numbered up *ad infinitum* to generate unlimited amounts of nanomaterial, the successful numbering up of microfluidic devices to generate a gram of functionalized nanomaterials has not been demonstrated.[22,23,25,38] In addition, despite at least two recognized gram-scale AuNR batch syntheses being published, the development of a convenient gram-scale syntheses for functionalized gold nanoparticles remains a pressing challenge.[22,23,25] In contrast, the synthesis of a gram of gold nanorods with controlled aspect ratios in the millifluidic reactor can be achieved with no modifications to the original synthesis simply by running a single reactor continuously.

Based on the estimated yield of our standard gold nanorods synthesis within the flow reactor, we calculated that 10.0 L of the standard gold nanorod reaction solution would have to be prepared to generate 1.0 g of gold nanorods with aspect ratio 2.[18,48] Accordingly, three separate 3.30 L fractions were synthesized in sequence, and combined to make a single 10.0 L solution of synthesized gold nanorods. To synthesize 10 L of gold nanorods in solution, three hours were required to mix the appropriate volumes of growth and seed solutions in the millifluidic flow reactor. After exiting the reactor, the synthesized nanorod solution was a deep blue color, consistent with the formation of gold nanorods with AR ~ 2.[18,48]

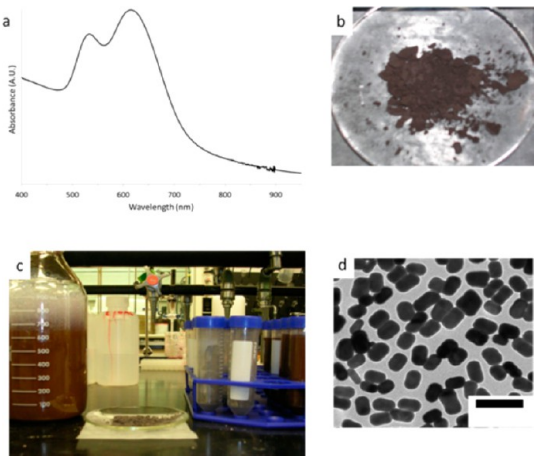

Figure 7. The high-throughput synthesis enabled by the flow reactor facilitates the synthesis of mondisperse gold nanorods on a gram scale in a matter of hours. (a) UV−vis absorbance spectrum of the low-aspect ratio gold nanorod solution. The sample has been diluted by a factor 10. (b) A sample of the lyophilized rods (103.6 mg, recovered from 100.0 mL of the AuNR solution) is shown. (c) Lyophilized rods and the concentrated gold nanorods solution. (d) TEM image of the AuNRs prepared in the gram-scale synthesis. Scale bar is 200 nm.

All 10.0 L of gold nanorod solution were purified and concentrated by centrifugation, and analyzed by UV−vis absorbance spectroscopy and TEM. Figure 7a,d shows UV−vis and TEM data for the gold nanorod solution. The UV−vis spectrum of the AuNR solution shown in Figure 7 is for the as-synthesized AuNR solution diluted 10 times. TEM analysis of the gram scale synthesis sample indicates that the solution is composed of low aspect ratio (AR = 1.83 ± 0.3) gold nanorods with dimensions of 79.6 ± 10.1 × 44.5 ± 6.9 nm ($N = 50$). The gold nanorods in this sample show good monodispersity, as can be seen in the TEM images (Figure 7, Supporting Information Figure S9).

On the basis of the UV−vis absorbance data, it was estimated that we had synthesized 1.5 g of CTAB-stabilized gold nanorods.[18] To verify the yield of gold nanorods produced by this method, we purified the gold nanorods by centrifugation and concentrated the solution by a factor of 10, then lyophilized a fraction of concentrated rod solution to determine a dry weight for the purified gold nanorods (the AuNRs produced by this method could also be successfully purified by diafiltration, Supporting Information). We found that 100.0 mL of the concentrated solution yielded 103.6 ± 0.7 mg of a dry red-purple powder (Figure 7b,c). This corresponds to an overall yield of 1.04 ± 0.02 g of CTAB-stabilized gold nanorods. Therefore, we have demonstrated that a gram of monodisperse gold nanorods can be produced within hours using our simple millifluidic reactor, yet close control over gold nanorod dimensions is maintained. In contrast, previously reported batch gram-scale AuNR syntheses require close monitoring and frequent adjustments to the timing of

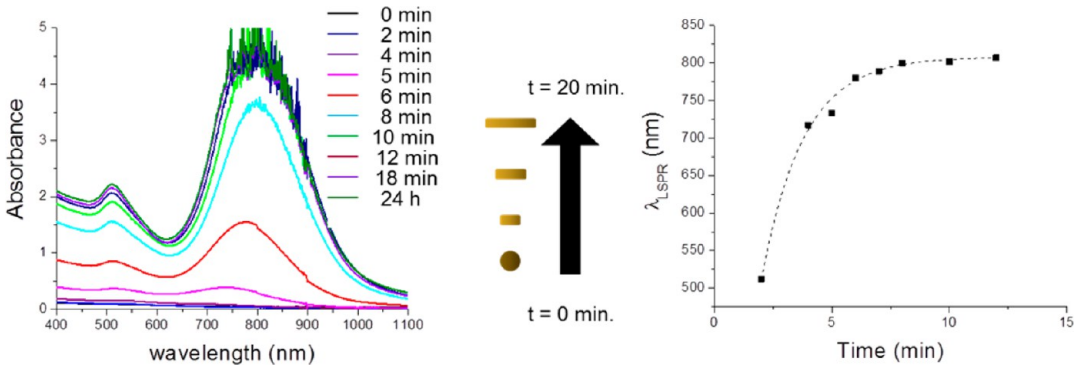

Figure 8. The millifluidic reactor provides an opportunity to monitor the growth of gold nanoparticles in real time. (a) UV−vis absorption spectra of borohydride-mediated AuNR growth, from 0 to 18 min residence time, along with a plot of the finished AuNRs at 24 h. (b) The corresponding plot of the longitudinal SPR λ_{max} *versus* time over the first 15 min for growth of the "small" AuNRs. Standard errors are shown, but are less than the width of the data points.

reagent addition, temperature, etc. to maintain appropriate aspect ratio control during synthesis.[22,23]

Integrated Real-Time Optical Analysis of Gold Nanoparticle Products. The millifluidic reactor also facilitates the real-time analysis of gold nanoparticle formation, by placing an in-line flow-through cuvette for UV−vis absorption spectroscopy analysis.[38,39,42] The observation cell can be placed at different distances from the mixer, providing an opportunity to monitor the steady-state AuNP population at different residence times, without interfering with AuNP synthesis.[42] The ability to monitor AuNP product formation in real-time potentially facilitates mechanistic investigations as well as applications for quality control during synthesis.[38,39,42] Monitoring the progress of AuNP synthesis within the fluidic environment provides an opportunity for researchers to reduce wasted material, as the synthesis can be stopped immediately if reaction conditions become inhomogeneous.[14,16,25]

To demonstrate the potential for real-time monitoring, we tracked the growth of small gold nanorods in the borohydride-mediated synthesis in real time using the millifluidic reactor.[22,50,51] Absorbance spectra of the AuNR solution were taken at different residence times: 2, 4, 6, 8, 10, 12, 15, and 18 min. These spectra were then compared to the spectrum of the "finished" AuNRs after 24 h Although the absorbance spectrum initially shows minimal absorbance features at two and four minute residence times, consistent with the formation of new nuclei (AuNPs < 2.0 nm), absorption features consistent with the formation of AuNRs begin to emerge by 6 min (Figure 8).[22] Ultimately, the transverse and longitudinal SPR peaks at approximately 510 and 780 nm, respectively, appeared, with anisotropic growth having essentially terminated after approximately 15 min reaction time (as supported by a plot of the LSPR λ_{max} over time Figure 8). Unlike the standard seeded growth synthesis of single-crystalline gold nanorods, these small gold nanorods displayed minimal blue-shift in the position of the longitudinal plasmon absorbance between 15 min and 24 h of growth, suggesting that after 15 min, these small AuNRs have grown to their full aspect ratio, and then experience no subsequent isotropic growth.[22,57] While the peristaltic pump used to drive synthesis in this millifluidic reactor is perhaps not ideal for detailed mechanistic investigations (nor is this system optimized for detailed kinetic studies or rapid AuNP growth reactions, possessing a limited time resolution of 4.6 s),[42] we anticipate that similar millifluidic reactors that employ more narrow volume channels/observation cells, while being powered by pumps that provide more consistent and controlled pressure (such as syringe pumps) might be ideal platforms for the mechanistic investigation of many different types of nanoparticle growth.[42]

We also tested the potential of this real time monitoring approach for quality control during AuNR synthesis. Using the standard silver-assisted seeded growth synthesis for AuNRs,[15,18,48] we spiked the gold nanorod growth solution with excess ascorbic acid (∼an additional 22.0 μL of 0.1 M ascorbic acid per 100.0 mL of sample volume), and set the observation cell at 15 min residence time to see if we could observe the formation of unwanted byproducts. We observed the presence of an impurity in the product at this residence time (likely corresponding to the formation of unwanted low-aspect ratio AuNRs in the reaction mixture, Figure 9). The presence of these unwanted byproducts is evidenced by a decrease in the intensity of the longitudinal LSPR peak at ∼780 nm, and the emergence of an additional plasmon absorbance at ∼580 nm. By monitoring the AuNR sample at either wavelength (575 or 780 nm), the quality of the AuNR product can be assessed in real time (Figure 9). After observing the formation of this unwanted byproduct by UV−vis, we immediately stopped the reactor, and rinsed the system with nanopure water. We prepared a new gold nanorod growth solution (containing the correct amount of ascorbic acid), and resumed observation of the growth solution at 15 min residence time. This time, the desired pristine gold nanorod sample

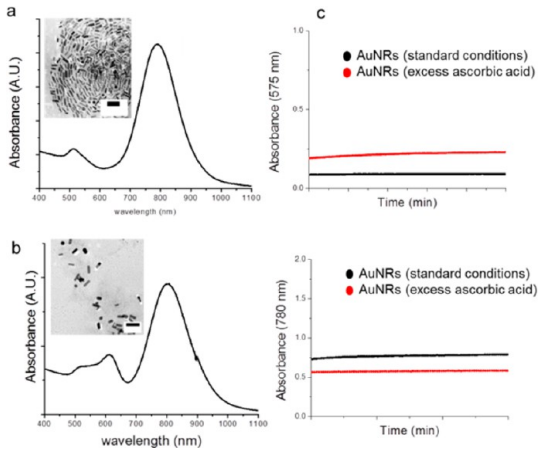

Figure 9. In-line UV−vis absorbance monitoring can also be used for quality control purposes. UV−vis absorbance spectra and TEM images for AuNRs synthesized under standard (a) *versus* AuNR products obtained from a growth solution containing too much ascorbic acid (b). The presence of the unwanted short AuNR byproducts can also be identified by monitoring the absorbance over time at two key diagnostic wavelengths: 575 nm and 780 nm (c).

was observed, as the UV−vis absorbance spectrum showed no evidence of unwanted byproducts. The presence and absence of unwanted low AR AuNR byproducts in the product sample were confirmed by TEM analysis (Figure 9). This simple experiment shows how the millifluidic reactor can facilitate real-time monitoring of the AuNP products during synthesis, providing an opportunity to avoid wasted reagents and materials, particularly during gram-scale synthesis in the reactor.

High-Throughput Functionalization of Gold Nanorods Using Tangential Flow Filtration. In the past decade, a variety of techniques have been developed for the functionalization of gold nanoparticles, including ligand exchange with bulky thiols and phosphines, layer-by-layer (LBL) polyelectrolyte wrapping, and silica coating.[4,16,21,44,56] While most of these techniques readily facilitate the functionalization of milligram scale quantities of material, the functionalization of larger quantities of material remains a significant challenge, primarily because purification in these procedures is typically accomplished using low-throughput procedures, such as chromatography, centrifugation, dialysis, or solvent washing.[14,44] Consequently, the development of high-throughput nanoparticle purification techniques has recently become the subject of significant research.[14,44] We anticipated that one such technique (tangential flow filtration, TFF) could easily be integrated into our capillary flow reactor system to provide an opportunity for scalable, high-throughput gold nanoparticle functionalization that could be integrated with the millifluidic reactor.[44] Purification by tangential flow filtration (aka *diafiltration*) could be incorporated into the reactor, simply by adding an additional peristaltic pump (with a TFF filtration cassette attached) in-line after AuNP synthesis was complete.

We explored the utility of TFF (integrated into our millifluidic reactor) as a purification technique to facilitate high-throughput nanoparticle functionalization/purification in three separate instances: the removal of CTAB and small AuNP byproducts from the crude reaction product of gold nanorods synthesis, gold nanorod functionalization using LBL polyelectrolyte wrapping,[55] and thiol exchange on gold nanorods. The TFF setup is shown in Figure 1c. This TFF purification configuration is essentially identical to the setup described by Sweeney et al. in 2006.[44] In each of these cases, the crude gold nanorod solution to be purified is added to the retentate reservoir, and then the sample is purified by passing 40.0 volume equivalents of eluent through the system.[44] Gold nanorod purity is assessed by a combination of UV−vis absorption analysis, ζ-potential analysis, FTIR, XPS, and TGA. The results of the LBL functionalization of gold nanorods using TFF purification is described below, while the removal of excess CTAB from crude AuNR synthetic mixtures, and mPEG exchange are described in the Supporting Information.

LBL polyelectrolyte wrapping of AuNRs was accomplished using a modified version of our previously reported standard polyelectrolyte wrapping procedure (which has previously been optimized for wrapping time and polyelectrolyte concentration).[55] In our optimized procedure, excess CTAB was first removed from the AuNR synthetic solution either by TFF or centrifugation.[55] Next, the purified AuNRs were then concentrated and resuspended in a 1.0 mM NaCl solution. The first polyelectrolyte (sodium polyacrylate, PAA [15 000 g/mol], 10 mg/mL in 1.0 mM NaCl) was then added to initiate wrapping, and was allowed to stir with the AuNRs for approximately 30 min.[55] Following this wrapping stage, purification by TFF was begun. After purification, polyelectrolyte wrapping with the next polyelectrolyte, polyallylamine hydrochloride (PAH, M_w 15 000 g/mol), was initiated.

TFF purification is driven by a peristaltic pump attached to a commercially available diafiltration membrane. The polyelectrolyte wrapping solution is placed in the syringe, and the excess polyelectrolyte is removed by continuously circulating the AuNR solution (retentate) through the diafiltration membrane, while impurities are removed into the filtrate stream.[44] The eluent in this purification procedure is 1.0 mM NaCl, which is added to the retentate periodically to preserve a constant volume. The AuNP solution is "pure" (*i.e.*, ready for the next PE wrapping stage) after 20.0 vol equiv of NaCl (relative to the initial PE wrapping solution volume) have been passed through the membrane.[44] For example, to purify 20.0 mL of AuNR-PE solution, 400.0 mL of NaCl solution must be passed through the membrane.

We successfully wrapped AuNRs with five layers of polyelectrolyte (PAA-PAH-PAA-PAH-PAA), using this

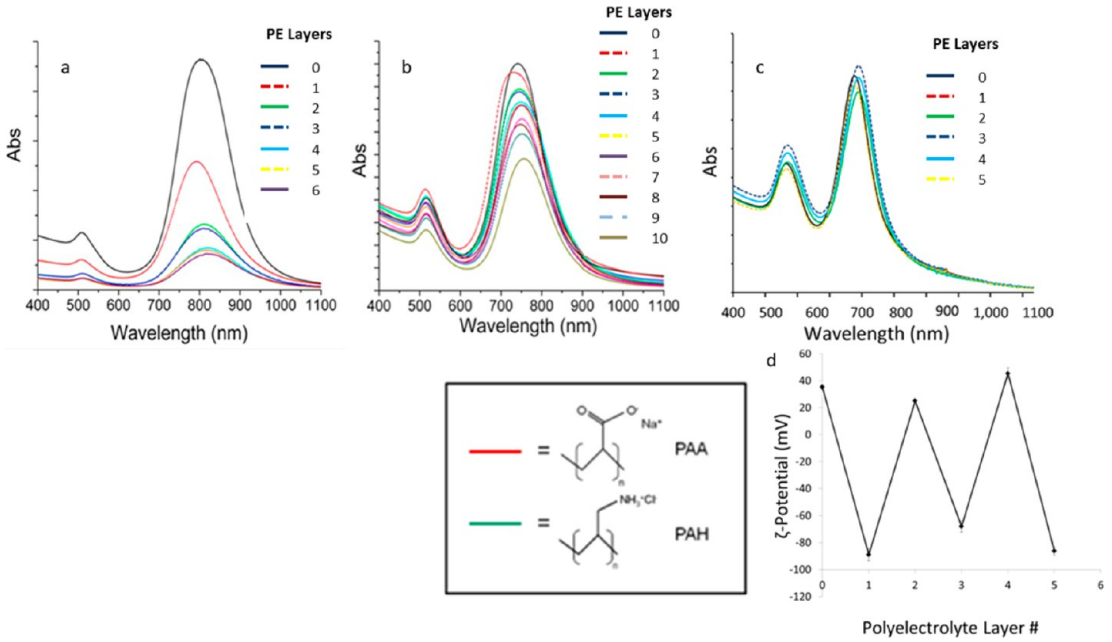

Figure 10. Functionalized gold nanorod purification in flow provides superior throughput *versus* standard purification approaches like centrifugation, as well as reducing product loss. (a) UV−vis absorbance analysis shows that, for AuNRs functionalized using our previously reported layer-by-layer wrapping approach (purified by centrifugation), significant product loss becomes apparent after just one layer of wrapping. (b) Our optimized layer-by-layer wrapping procedure minimizes product loss during centrifugation, but reduces throughput. Still, significant losses are observed after just three layers of AuNR wrapping. (c) Using tangential flow filtration, gold nanorods can be quickly purified during the LBL-wrapping procedure, and minimal product loss occurs, even after five layers of PE wrapping. (d) ζ-Potential analysis indicates that, after each purification stage by TFF, the gold nanorods are well protected by the new layer of polyelectrolyte.

TFF-driven approach. The UV−vis absorbance spectrum of the AuNR solution following each wrapping stage is shown in Figure 10. The change in the λ_{max} for the LSPR after each PE layer suggests that wrapping was successful at each stage. This was further confirmed by ζ-potential analysis of the AuNR solutions (Figure 10d). Each wrapping cycle requires three-six hours to complete (including both wrapping and purification), depending on the volume of solution that must be purified.

We compared the LBL wrapping of functionalized AuNRs with purification driven by diafiltration to our traditional wrapping procedure (with purification by centrifugation)[55] as well an optimized LBL procedure we recently developed in which the solutions are purified using longer centrifugation runs at slower speeds or dialysis. Using our original protocol for centrifugation-based LBL wrapping of AuNRs, a single wrapping cycle takes approximately 4 h to complete; however, significant product loss is observed even after the first wrapping stage, due to AuNR aggregation (Figure 10a).[55] Using the new optimized wrapping procedure (although still using dialysis/centrifugation for purification), each layer requires approximately 26 h to complete, but product loss is significantly reduced *versus* the original procedure (Figure 10b).[55]

Polyelectrolyte wrapping with purification using TFF provides improved throughput in most cases *versus* polyelectrolyte wrapping using purification by centrifugation or dialysis. Typically, LBL purification by centrifugation or dialysis is a low-throughput procedure which limits the throughput to a maximum of ∼0.005 mg/min AuNRs.

In contrast, purification by TFF is scalable, and in principle, any volume of AuNR solution can be accommodated by this apparatus.[44] Based on the UV−vis data obtained for Figure 10, we estimate the throughput of purification by TFF to be 0.76 mg/min, orders of magnitude faster than purification by centrifugation or dialysis.[18] Furthermore, TFF offers a mild purification approach that reduces product losses due to aggregation, because the AuNPs are not forced into close physical contact during purification. Accordingly, the UV−vis absorbance spectrum of the AuNR solution after each wrapping stage shows no evidence of significant product loss after the first five wrapping stages.[55]

Polyelectrolyte wrapping with purification by TFF also results in reduced loss of product compared to purification by centrifugation. UV−vis absorbance analysis of the AuNR product after five PE wrapping stages PAA-PAH-PAA-PAH-PAA shows no significant loss of product over the course of the five purification stages.[18] In comparison, purification using our original centrifugation protocol generally results in the loss of nearly one-quarter of the nanorods by the third LBL wrapping stage (Figure 10a). The amount of product lost using the TFF procedure is even slightly less than the amount of product lost using an

optimized centrifugation protocol (Figure 10b), while providing superior throughput. Therefore, we conclude that purification by TFF during polyelectrolyte wrapping not only provides improved throughput and scalability during purification, but is also a milder purification technique, reducing the amount of product lost during the wrapping stages.

CONCLUSIONS

We have shown that a millifluidic reactor for hydrophilic functionalized AuNP synthesis can be assembled entirely from commercially available components that can be found in almost any chemistry laboratory. This reactor permits the high-throughput synthesis of functionalized gold nanoparticles with controlled sizes and shapes, which provides a facile means to prepare monodisperse gold nanoparticles on the gram scale. We have shown that the synthesis of gold nanorods in the reactor can be fine-tuned to control gold nanorod aspect ratios, and also alter the absolute dimensions of the gold nanorods. For instance, the dimensions of the gold nanorods can be deliberately coarsened within the flow reactor to provide "fat" gold nanorods, as well as "small" gold nanorods (AuNRs with absolute dimensions smaller than are typically achieved in seeded growth). The reactor can also be easily integrated with UV−vis absorbance spectroscopy analysis to provide real time analysis of the AuNP product for quality control purposes. The reactor can further be integrated with tangential flow filtration to provide an integrated high-throughput AuNR functionalization platform. Our millifluidic reactor represents a versatile, portable high-throughput gold nanoparticle production device that can be assembled and operated by individual researchers in any laboratory in order to reproducibly synthesize gram-scale quantities of functionalized gold nanoparticles or possibly facilitate high-throughput method development.

We would like to emphasize that while the millifluidic device described here provides some significant advantages in high-throughput AuNP synthesis, particularly for individual research laboratories, the reactor design that we described here is very much a "version 1.0" model. The current design of the reactor is deliberately open-ended and flexible, opening possibilities for further reactor modifications that may provide ever greater control over NP properties during synthesis (the use of simulations to guide new mixer designs, *etc.* may be particularly useful in this regard).[58,59] In addition, because the reactor we describe is compatible with a wide variety of AuNP syntheses, recent improvements in batch AuNP synthetic chemistry will make it even easier to synthesize more monodisperse AuNPs at higher concentrations in the reactor.[24] Ultimately, our hope is that this demonstration of the construction and operation of a simple millifluidic reactor for AuNP synthesis may inspire other researchers to design analogous reactors for their own NP synthesis purposes.

MATERIALS AND METHODS

Materials. All materials were used as received, unless otherwise noted. Gold tetrachloroaurate trihydrate ($HAuCl_4 \cdot 3H_2O$), 6-mercaptohexanoic acid (MHA), sodium borohydride ($NaBH_4$), sodium polyacrylate (30 wt % solution, M_w 15 000 g/mol, PAA), polyallylamine hydrochloride (M_w 15 000 g/mol PAH), and silver nitrate ($AgNO_3$) were obtained from Sigma Aldrich. Hexadecyltrimethyl ammonium bromide (CTAB), L-ascorbic acid, and trisodium citrate were obtained from Sigma. mPEG (M_w 5000 kDa) was obtained from NANOCS. Deionized water was prepared using a Barnstead NANOPURE water filter. PALL Minimate tangential flow filtration capsules for AuNP purification, with pore sizes between 10 and 300 kDa, were obtained from VWR. Two types of TEM grids, SiO on copper mesh (PELCO) and amine-functionalized Si/SiN SMART GRIDS (Dune Sciences), were used for transmission electron microscopy studies. The millifluidic reactor was assembled from commercially available components: a peristaltic pump (Cole-Palmer Masterflex L/S), Tygon polyvinyl tubing (i.d. = 2.79 mm), polyethylene Y-mixers (i.d. = 1.79 mm), and joints. A 3.0 mL flow-through UV−vis observation cell was obtained from Starna.

Flow Reactor Assembly and Operation for Gold Nanoparticle Synthesis. The capillary flow reactor was assembled from a peristaltic pump (Cole-Palmer Masterflex L/S), TYGON polyvinyl tubing, and polyethylene mixers and joints as shown in Figure 1. During synthesis, the reactor was operated at an overall flow rate of approximately 50.0 mL/min, which was found to be the optimal flow rate for nanoparticle synthesis (Supporting Information, Figure S1). For the majority of gold nanoparticle syntheses, the reactor was assembled with sufficient tubing (540.0 cm) to give a residence time in the reactor of 3.0 min. However, for seeded growth syntheses, a residence time of 15.0−20.0 min was typically used; this residence time provides sufficient time for size evolution to be completed in the seeded growth of spheres, and for anisotropic growth to be completed in the synthesis of gold nanorods (Supporting Information, Figures S3, S4). Following elution from the reactor, the AuNP solution is collected in an aqua regia-cleaned 500.0 mL Erlenmeyer flask with stirring, and is held in the collection flask for 2−3 h prior to characterization or functionalization. Additional details regarding the construction of the flow reactor, mixing in the flow reactor, and the determination of the optimal flow rate for synthesis can be found in the Supporting Information. Prior to synthesis, growth solutions, seed solutions, and sodium borohydride solutions were stored in Corningware tubes or aqua regia-cleaned Erlenmeyer flasks.

Gold Nanoparticle Synthesis in the Millifluidic Reactor. *Synthesis of 4.0 nm Citrate-Stabilized AuNP.* Citrate-stabilized AuNPs were synthesized using a modified version of previously reported synthetic procedures.[16,20] Briefly, 200.0 mL of a growth solution, 2.0 mM in gold tetrachloraurate ($HAuCl_4$) and 6.0 mM in sodium citrate, and 200.0 mL of a 5.0 mM aqueous sodium borohydride solution were prepared. The two solutions were flowed together in the reactor at a flow rate of 50.0 mL/min, and experienced a residence time of 3.0 min. The combined solutions rapidly change color to a deep brown, and then red-brown prior to exiting the reactor. The AuNP solution was collected in an aqua regia-cleaned 500.0 mL Erlenmeyer flask, and stirred for 3.0 h.

Synthesis of 3.0 nm Mecraptohexanoic Acid (MHA)-Stabilized AuNPs. MHA-stabilized AuNPs were synthesized using a variation of the Brust-Schiffrin procedure.[16,44,46,47] Briefly, 200.0 mL of a growth solution was prepared: 3.0 mM in $HAuCl_4$ and

6.0 mM in MHA in nanopure deionized water. Then, 200.0 mL of an aqueous 5.0 mM $NaBH_4$ solution was also prepared. The two solutions were flowed together at 50.0 mL/min in the reactor, and experienced a residence time of 3.0 min. The combined solutions rapidly change color to a deep brown. The AuNP solution was collected in an aqua regia-cleaned 500.0 mL Erlenmeyer flask, and stirred for 3.0 h.

CTAB-Stabilized AuNP Synthesis. CTAB-stabilized AuNPs were prepared using a modification of previously reported seeded growth procedures.[45] All solutions were flowed through the pump system at a flow rate of 50.0 mL/min. Residence time was 3.0 min.

Synthesis of 2.0 nm CTAB-Stabilized AuNPs. A growth solution was prepared containing 10.0 mM $HAuCl_4$ and 200.0 mM CTAB in 200.0 mL nanopure deionized water. This was combined with 200.0 mL of an aqueous 5.0 mM $NaBH_4$ solution. The combination of these solutions rapidly produces a deep brown solution.

Synthesis of 8.0 nm CTAB-Stabilized AuNPs. A growth solution was prepared: 10.0 mM in $HAuCl_4$ and 200.0 mM in CTAB in 200.0 mL nanopure deionized water. This was combined with 200.0 mL of an aqueous 0.02 mM $NaBH_4$ solution. The combination of these solutions rapidly produces a vibrant red solution.

Synthesis of 20.0 nm CTAB-Stabilized AuNPs. The 8.0 nm CTAB-stabilized AuNPs were used as seeds in the synthesis of larger AuNPs. Briefly, 20.0 nm CTAB-AuNPs were prepared by combining a solution of 8.0 nm CTAB-stabilized AuNPs [(see above, purified by centrifugation) by dissolving 10.0 mL of this solution in 50.0 mL of nanopure deionized water], with a growth solution (50.0 mL) containing 1.0 mM $HAuCl_4$, 0.1 M CTAB, and 2.0 mM ascorbic acid. Shortly after mixing, the reaction solution turns from a clear, colorless solution to a vibrant red solution.

Synthesis of 40.0 nm CTAB-Stabilized AuNPs. The 20.0 nm CTAB-stabilized AuNPs were used as seeds in the synthesis of larger AuNPs. Briefly, 40.0 nm CTAB-AuNPs were prepared by preparing a solution of 20.0 nm CTAB-stabilized AuNPs (see above, purified by centrifugation) by dissolving 10.0 mL of this solution in 50.0 mL of nanopure deionized water]. This was added to a growth solution containing 1.0 mM $HAuCl_4$, 0.1 M CTAB, and 2.0 mM ascorbic acid. Shortly after mixing, the reaction solution turns from a clear, colorless solution to a deep red-purple solution.

Synthesis of Gold Nanorods Using a Seeded Growth Approach in the Flow Reactor. Gold nanorods with aspect ratios between 1.5 and 4.0 were synthesized using our previously reported seeded growth procedures.[15,18,48] Two solutions were prepared, labeled "Growth" and "Seed." For the growth solution, 1.25 mL $HAuCl_4$ (0.01 M), 55.0−250.0 μL $AgNO_3$ (0.01 M), and 137.5 μL L-ascorbic acid (0.1 M) were added to a 0.1 M aqueous CTAB solution with a final volume of 12.5 mL. For the seed solution, 30.0 μL of a gold nanoparticle seed dispersion (aged 2 h) was added to 12.5 mL CTAB (0.1 M). The solutions were mixed within the flow reactor (flow rate = 50 mL/min), and the AuNR growth solution experiences a residence time of approximately 15.0 min in the reactor before depositing into a 50 mL conical tube.

Synthesis of Small Gold Nanorods Prepared by the "Seedless" (Borohydride-Assisted) Method in Flow Reactor. The synthesis of small gold nanorods was performed based on previously reported procedures.[22,49,50] Two 25.0 mL solutions were prepared, labeled "Growth" and "Borohydride." For the growth solution, 0.5 mL $HAuCl_4$ (0.1 M) and 3.75 mL $AgNO_3$ (0.02 M) were added to 20.75 mL of CTAB (0.1 M). The mixture was then mildly heated until no longer turbid, then cooled to room temperature before 0.5 mL of L-ascorbic acid (0.2 M) was added. The growth solution was shaken until clear. For the sodium borohydride solution, 50−1700 μL of $NaBH_4$ (0.045 mM) was added to 29.95−23.30 mL of nanopure deionized water. The solutions were mixed together *via* the flow reactor at 50.0 mL/min and were held in the capillary flow reactor for a residence time of 10.0 min, before being deposited into a 50.0 mL conical tube while stirring.

Synthesis of Seeded "Fat" Gold Nanorods in Flow Reactor. Gold nanorods which have been modified by isotropic overgrowth to yield dog-boned gold nanorods and gold nanorods with large transverse diameters were prepared by increased ascorbic acid addition.[51−53] Two solutions were prepared, labeled "Growth" and "Seed." For the growth solution, 18.6 mL of CTAB (0.1 M), 5.0 mL of $HAuCl_4$ (0.0 1M), 0.75 mL of $AgNO_3$ (0.01 M) were combined and homogenized. Then, 0.63 mL of L-ascorbic acid (0.1 M, 1.4 mol equiv relative to $HAuCl_4$) were added, and the container was shaken until clear. For the Seed solution, 50−400 μL of 4.0 nm gold seed dispersion (aged 2 h) was added to 25 mL of CTAB (0.1 M). The solutions were combined in the flow reactor at 50 mL/min before depositing in to a 50 mL conical tube. Typical nanorod concentration was 1.2 nM as synthesized.

Gram Scale Synthesis of Gold Nanorods. The gram scale synthesis of gold nanorods was achieved by using the standard conditions for gold nanorods synthesis, and the AuNRs were continuously synthesized until approximately 1 g of material (estimated based on concentration determined by UV−vis absorbance spectroscopy) has been produced. The synthesis of 1 g of gold nanorods was subdivided into three 3.3 L synthesis runs (final AuNR concentration of 1.0 nM). For each synthesis, 125 mL of $HAuCl_4$ (0.01 M) was combined with 5.5 μL of $AgNO_3$ (0.01 M), and 137.5 mL of L-ascorbic acid (0.1 M) was added to a 0.1 M aqueous CTAB solution with a final volume of 1.65 L. For the Seed solution, 3.0 mL of a gold nanoparticle seed dispersion (aged 2 h) was added to 1.65 mL of CTAB (0.1 M). The solutions were mixed in the reactor at a constant flow rate of 50.0 mL/min, and the reaction solution experienced a residence time of 20 min within the reactor before the resultant blue solution was deposited into an aqua regia-cleaned 5.0 L Erlenmeyer flask with stirring. The solution was stirred overnight prior to purification.

Purification and Functionalization of Gold Nanorods. *AuNP Purification by Tangential Flow Filtration (TFF).* Following synthesis, gold nanoparticle solutions were purified using one of two methods, either by centrifugation or using tangential flow filtration[44] to remove unwanted small AuNP byproducts and free ligands (*e.g.*, thiols, CTAB, or citrate). Purification by TFF requires the passage of 20−40 volume equivalents of nanopure through the TFF membrane. CTAB-AuNR solutions could alternately be purified by centrifugation (2×, 14 000 RCF, 10 min).

Thiol Exchange and Polyelectrolyte Wrapping with Purification Driven by TFF. For polyelectrolyte wrapping, the purified AuNR solution was resuspended in 1.0 mM NaCl, and wrapped by incubation with 10.0 mg/mL polyelectrolyte solution (either PAA or PAH, depending on the desired layer).[55] The wrapping solution was stirred for 1 h in a 60.0 mL Corningware tube. A separate TFF membrane cassette is used for each type of polyelectrolyte layer (*i.e.*, separate TFF assemblies for the purification of positively and negatively charged PE-AuNR solutions). Following polyelectrolyte wrapping, the functionalized gold nanorod solution is added to the TFF membrane and purified by diafiltration with 20 vol equiv of 1.0 mM NaCl. Following purification, the purified gold nanorods solution is resuspended in 1.0 mM NaCl solution and the polyelectrolyte wrapping procedure is repeated with the subsequent layer. Once five cycles of wrapping have been completed, the finished polyelectrolyte-wrapped rods are additionally purified by diafiltration with 20 volume equivalents of nanopure.

mPEG Thiol Exchange Driven by Diafiltration. For mPEG thiol exchange, the purified CTAB-AuNRs were added to a 4 mg/mL solution of $mPEG_{(aq)}$, and the solution was stirred for 24 h. At this time, the crude mPEG-AuNR solution is transferred to the diafiltration apparatus and purified by passing 20 vol equiv of nanopure through the diafiltration apparatus.

Real-Time Analysis of AuNP Growth. To analyze the growth of AuNPs in real time, a quartz-walled flow-through observation cell (Starna) was placed at different distances (corresponding to specific residence times between 1 and 30 min.) from the mixer and the reaction mixture was analyzed continuously at that residence time using an HP diode array spectrophotometer. The total volume of the flow cell was 4.0 mL and the UV−vis time resolution of the current system was found to be 4.6 s, based on the volume of solution required to refresh the observation cell.[42] The syntheses were performed under the standard reaction conditions described above.

Real-Time Quality Control During AuNR Synthesis. A standard gold nanorod growth solution was prepared, but spiked with a small additional aliquot of ascorbic acid (160.0 μL *versus* 137.5 μL), to deliberately prepare a gold nanorod sample with unwanted impurities. The synthesis was run in the reactor under the standard conditions described above, and the solution was analyzed by UV−vis absorbance spectroscopy at a residence time of 15 min. The UV−vis absorbance spectroscopy analysis revealed the presence of an unwanted byproduct in the reaction mixture. At this time, the flow of the reaction solution through the reactor was stopped, and the reactor was rinsed with 200.0 mL of nanopure deionized water. The growth solution was then replaced with a growth solution containing the standard amount of ascorbic acid. Stopping the reactor, remixing the growth solution, rinsing the reactor, and restarting the synthesis took approximately 17 min. The new reaction solution continued to be monitored by UV−vis absorbance at 15 min to ensure the quality of the AuNR solution.

Functionalized Gold Nanoparticle Characterization and Analysis. Gold nanorod solutions were analyzed using a combination of UV−vis absorption spectroscopy, transmission electron microscopy (TEM), ζ-potential analysis, FTIR, and X-ray photoelectron spectroscopy (XPS). UV−vis absorbance spectroscopy analysis was performed using a Cary 500 Scan UV−vis-NIR Spectrophotometer. For transmission electron microscopy analysis, a small aliquot of the purified AuNP solution was dropcast onto a SiO/Cu mesh/Formvar TEM grid (Ted Pella), and examined using a JEOL 2100 Cryo TEM. Size distributions for the AuNPs were determined using ImageJ analysis, according to previously reported procedures.[56] For XPS analysis, purified AuNP solutions were dropcast onto indium foil and analyzed using a Kratos Axis Ultra XPS, with a monochromated Al X-ray source. For FTIR analysis, purified AuNP solutions were dropcast onto a PTFE IR analysis card, and analyzed using a Thermo Nicolet 6700 FTIR Spectrometer.

Conflict of Interest: The authors declare no competing financial interest.

Supporting Information Available: Additional TEM images, surface analysis data for the AuNPs synthesized in the flow reactor, a more detailed description of the reactor construction and operation. This material is available free of charge *via* the Internet at http://pubs.acs.org.

Acknowledgment. The authors gratefully acknowledge the assistance of the Yi Lu research group at the Department of Chemistry, University of Illinois Urbana−Champaign, for assistance with real-time UV−vis absorbance analysis. The authors furthermore thank the staff of the Frederick Seitz Material Research Facility at the University of Illinois for assistance with surface chemistry analysis. This material is based upon work supported by the National Science Foundation under the Center for Sustainable Nanotechnology, CHE-1240151.

REFERENCES AND NOTES

1. Huang, X. H.; Neretina, S.; El-Sayed, M. A. Gold Nanorods: From Synthesis and Properties to Biological and Biomedical Applications. *Adv. Mater.* **2009**, *21*, 4880–4910.
2. Kooij, E. S.; Poelsema, B. Shape and Size Effects in the Optical Properties of Metallic Nanorods. *Phys. Chem. Chem. Phys.* **2006**, *8*, 3349–3357.
3. Sardar, R.; Funston, A. M.; Mulvaney, P.; Murray, R. W. Gold Nanoparticles: Past, Present, and Future. *Langmuir* **2009**, *25*, 13840–13851.
4. Lohse, S. E.; Murphy, C. J. Applications of Colloidal Inorganic Nanoparticles: From Medicine to Energy. *J. Am. Chem. Soc.* **2012**, *134*, 15607–15620.
5. Dickerson, E. B.; Dreaden, E. C.; Huang, X. H.; El-Sayed, I. H.; Chu, H. H.; Pushpanketh, S.; McDonald, J. F.; El-Sayed, M. A. Gold Nanorod Assisted Near-Infrared Plasmonic Photothermal Therapy (PPTT) of Squamous Cell Carcinoma in Mice. *Cancer Lett.* **2008**, *269*, 57–66.
6. Hribar, K. C.; Lee, M. H.; Lee, D.; Burdick, J. A. Enhanced Release of Small Molecules from Near-Infrared Light Responsive Polymer-Nanorod Composites. *ACS Nano* **2011**, *5*, 2948–2956.
7. Huang, H. C.; Rege, K.; Heys, J. J. Spatiotemporal Temperature Distribution and Cancer Cell Death in Response to Extracellular Hyperthermia Induced by Gold Nanorods. *ACS Nano* **2010**, *4*, 2892–2900.
8. Huang, Y. J.; Kim, D. H. Dark-Field Microscopy Studies of Polarization-Dependent Plasmonic Resonance of Single Gold Nanorods: Rainbow Nanoparticles. *Nanoscale* **2011**, *3*, 3228–3232.
9. Nusz, G. J.; Marinakos, S. M.; Curry, A. C.; Dahlin, A.; Hook, F.; Wax, A.; Chilkoti, A. Label-Free Plasmonic Detection of Biomolecular Binding by a Single Gold Nanorod. *Anal. Chem.* **2008**, *80*, 984–989.
10. Hao, L. L.; Patel, P. C.; Alhasan, A. H.; Giljohann, D. A.; Mirkin, C. A. Nucleic Acid-Gold Nanoparticle Conjugates as Mimics of microRNA. *Small* **2011**, *7*, 3158–3162.
11. Cutler, J. I.; Zhang, K.; Zheng, D.; Auyeung, E.; Prigodich, A. E.; Mirkin, C. A. Polyvalent Nucleic Acid Nanostructures. *J. Am. Chem. Soc.* **2011**, *133*, 9254–9257.
12. Jones, M. R.; Millstone, J. E.; Giljohann, D. A.; Seferos, D. S.; Young, K. L.; Mirkin, C. A. Plasmonically Controlled Nucleic Acid Dehybridization with Gold Nanoprisms. *Chem. Phys. Chem.* **2009**, *10*, 1461–1465.
13. Hill, H. D.; Mirkin, C. A. The Bio-Barcode Assay for the Detection of Protein and Nucleic Acid Targets Using DTT-Induced Ligand Exchange. *Nat. Protoc.* **2006**, *1*, 324–336.
14. Hutchison, J. E. Greener Nanoscience: A Proactive Approach to Advancing Applications and Reducing Implications of Nanotechnology. *ACS Nano* **2008**, *2*, 395–402.
15. Murphy, C. J. Sustainability as an Emerging Design Criterion in Nanoparticle Synthesis and Applications. *J. Mater. Chem.* **2008**, *18*, 2173–2176.
16. Dahl, J. A.; Maddux, B. L. S.; Hutchison, J. E. Toward Greener Nanosynthesis. *Chem. Rev.* **2007**, *107*, 2228–2269.
17. Crist, R. M.; Grossman, J. H.; Patri, A. K.; Stern, S. T.; Dobrovskaia, M. A.; Adiseshaiah, P. P.; Clogston, J. D.; McNeil, S. E. Common Pitfalls in Nanotechnology: Lessons Learned from NCI's Nanotechnology Characterization Laboratory. *Integr. Biol.* **2013**, *5*, 66–73.
18. Orendorff, C. J.; Murphy, C. J. Quantitation of Metal Content in the Silver-Assisted Growth of Gold Nanorods. *J. Phys. Chem. B* **2006**, *110*, 3990–3994.
19. Gao, J. X.; Bender, C. M.; Murphy, C. J. Dependence of the Gold Nanorod Aspect Ratio on the Nature of the Directing Surfactant in Aqueous Solution. *Langmuir* **2003**, *19*, 9065–9070.
20. Gole, A.; Murphy, C. J. Seed-Mediated Synthesis of Gold Nanorods: Role of the Size and Nature of the Seed. *Chem. Mater.* **2004**, *16*, 3633–3640.
21. Dreaden, E. C.; Alkilany, A. M.; Huang, X. H.; Murphy, C. J.; El-Sayed, M. A. The Golden Age: Gold Nanoparticles for Biomedicine. *Chem. Soc. Rev.* **2012**, *41*, 2740–2779.
22. Jana, N. R. Gram-Scale Synthesis of Soluble, Near-Monodisperse Gold Nanorods and Other Anisotropic Nanoparticles. *Small* **2005**, *1*, 875–882.
23. Alvarez-Puebla, R. A.; Agarwal, A.; Manna, P.; Khanal, B. P.; Aldeanueva-Potel, P.; Carbo-Argibay, E.; Pazos-Perez, N.; Vigderman, L.; Zubarev, E. R.; Kotov, N. A.; *et al.* Gold Nanorods 3D-Supercrystals as Surface Enhanced Raman Scattering Spectroscopy Substrates for the Rapid Detection of Scrambled Prions. *Proc. Natl. Acad. Sci. U.S.A.* **2011**, *108*, 8157–8161.
24. Ye, X.; Jin, L.; Cagalayan, H.; Chen, J.; Xing, G.; Zheng, C.; Doan-Nguyen, V.; Kang, Y.; Engheta, N.; Kagan, C. R.; *et al.* Improved Size-Tunable Synthesis of Monodisperse Gold Nanorods through the Use of Aromatic Additives. *ACS Nano* **2012**, *6*, 2804–2817.
25. Song, Y. J.; Hormes, J.; Kumar, C. S. S. R. Microfluidic Synthesis of Nanomaterials. *Small* **2008**, *4*, 698–711.
26. Bullen, C.; Latter, M. J.; D'Alonzo, N. J.; Willis, G. J.; Raston, C. L. A Seedless Approach to Continuous Flow Synthesis of Gold Nanorods. *Chem. Commun.* **2011**, *47*, 4123–4125.

27. Marre, S.; Jensen, K. F. Synthesis of Micro and Nanostructures in Microfluidic Systems. *Chem. Soc. Rev.* **2010**, *39*, 1183–1202.
28. Merkoci, A.; Kutter, J. P. Analytical Miniaturization and Nanotechnologies. *Lab Chip* **2012**, *12*, 1915–1916.
29. Boleininger, J.; Kurz, A.; Reuss, V.; Sonnichsen, C. Microfluidic Continuous Flow Synthesis of Rod-Shaped Gold and Silver Nanocrystals. *Phys. Chem. Chem. Phys.* **2006**, *8*, 3824–3827.
30. Nightingale, A. M.; de Mello, J. C. Microscale Synthesis of Quantum Dots. *J. Mater. Chem.* **2010**, *20*, 8454–8463.
31. Khan, S. A.; Duraiswamy, S. Controlling Bubbles Using Bubbles-Microfluidic Synthesis of Ultra-Small Gold Nanocrystals with Gas Evolving Reducing Agents. *Lab Chip* **2012**, *12*, 1807–1812.
32. Lazarus, L. L.; Riche, C. T.; Marin, B. C.; Gupat, M.; Malmstadt, N.; Brutchey, R. L. Two-Phase Microfluidic Droplet Flows of Ionic Liquids for the Synthesis of Gold and Silver Nanoparticles. *ACS Appl. Mater. Interfaces* **2012**, *4*, 3077–3083.
33. Hassam, A. A.; Sandre, O.; Cabuil, V.; Tabeling, P. Synthesis of Iron Oxide Nanoparticles in a Microfluidic Device: Preliminary Results in a Coaxial Flow Millichannel. *Chem. Commun.* **2008**, 1783–1785.
34. Duraiswamy, S.; Khan, S. A. Droplet-Based Microfluidic Synthesis of Anisotropic Metal Nanocrystals. *Small* **2009**, *5*, 2828–2834.
35. Yang, S. Y.; Cheng, F. Y.; Yeh, C. S.; Lee, G. B. Size-Controlled Synthesis of Gold Nanoparticles Using a Micro-Mixing System. *Microfluid. Nanofluid.* **2010**, *8*, 303–311.
36. Chan, E. M.; Alivisatos, A. P.; Mathies, R. A. High-Temperature Microfluidic Synthesis of CdSe Nanocrystals in Nanoliter Droplets. *J. Am. Chem. Soc.* **2005**, *127*, 13854–13861.
37. Richmond, C. J.; Miras, H. N.; de la Oliva, A. R.; Zang, H.; Sans, V.; Paramonov, L.; Makatsoris, C.; Inglis, R.; Brechin, E. K.; Long, D.-L.; *et al.* Flow-System Array for the Discovery and Scale Up of Inorganic Clusters. *Nat. Chem.* **2012**, *4*, 1037–1043.
38. Wagner, J.; Tshikhudo, T. R.; Koehler, J. M. Microfluidic Generation of Metal Nanoparticles by Borohydride Reduction. *Chem. Eng. J.* **2008**, *135*, S104–S109.
39. Biswas, S.; Miller, J. T.; Li, Y.; Nandakumar, K.; Kumar, C. S. S. R. Developing a Millifluidic Platform for the Synthesis of Ultrasmall Nanoclusters: Ultrasmall Copper Nanoclusters as a Case Study. *Small* **2012**, *8*, 688–698.
40. Li, Y.; Sanampudi, A.; Reddy, V. R.; Biswas, S.; Nandakumar, K.; Yemane, D.; Goettert, J.; Kumar, C. S. S. R. Size Evolution of Gold Nanoparticles in a Milllifluidic Reactor. *Chem. Phys. Chem.* **2012**, *13*, 177–182.
41. Jun, H.; Fabienne, T.; Florent, M.; Coulon, P.-E.; Nicolas, M.; Olivier, S. Understanding of the Size Control of Biocompatible Gold Nanoparticles in Millifluidic Channels. *Langmuir* **2012**, *28*, 15966–15974.
42. McKenzie, L. C.; Haben, P. M.; Kevan, S. D.; Hutchison, J. E. Determining Nanoparticle Size in Real Time by Small-Angle X-ray Scattering in a Microscale Flow System. *J. Phys. Chem. C* **2010**, *114*, 22055–22063.
43. Chan, E. M.; Xu, C.; Mao, A. W.; Han, G.; Owen, J. S.; Cohen, B. E.; Milliron, D. J. Reproducible, High-Throughput Synthesis of Colloidal Nanocrystals for Optimization in Multidimensional Parameter Space. *Nano Lett.* **2010**, *10*, 1874–1885.
44. Sweeney, S. F.; Woehrle, G. H.; Hutchison, J. E. Rapid Purification and Size Separation of Gold Nanoparticles *via* Diafiltration. *J. Am. Chem. Soc.* **2006**, *128*, 3190–3197.
45. Jana, N. R.; Gearheart, L.; Murphy, C. J. Seeding Growth for Size Control of 5−40 nm Diameter Gold Nanoparticles. *Langmuir* **2001**, *17*, 6782–6786.
46. Templeton, A. C.; Wuelfing, W. P.; Murray, R. W. Monolayer-Protected Cluster Molecules. *Acc. Chem. Res.* **2000**, *33*, 27–36.
47. Brust, M.; Walker, M.; Bethell, D.; Schiffrin, D. J.; Whyman, R. Synthesis of Thiol-Derivatised Gold Nanoparticles in a Two-Phase Liquid-Liquid System. *Chem. Commun.* **1994**, 801–802.
48. Sau, T. K.; Murphy, C. J. Seeded High Yield Synthesis of Short Au Nanorods in Aqueous Solution. *Langmuir* **2004**, *20*, 6414–6420.
49. Si, S.; Leduc, C.; Delville, M. H.; Lounis, B. Short Gold Nanorod Growth Revisited: The Critical Role of the Bromide Counterion. *Chem. Phys. Chem.* **2012**, *13*, 193–202.
50. Ali, M. R. K.; Snyder, B.; El-Sayed, M. A. Synthesis and Optical Properties of Small Au Nanorods Using a Seedless Growth Technique. *Langmuir* **2012**, *28*, 9807–9815.
51. Gou, L. F.; Murphy, C. J. Fine-Tuning the Shape of Gold Nanorods. *Chem. Mater.* **2005**, *17*, 3668–3672.
52. Ni, W.; Kou, X.; Yang, Z.; Wang, J. Tailoring Longitudinal Surface Plasmon Wavelengths, Scattering and Absorption Cross Sections of Gold Nanorods. *ACS Nano* **2008**, *2*, 677–686.
53. Song, J. H.; Kim, F.; Kim, D.; Yang, P. D. Crystal Overgrowth on Gold Nanorods: Tuning the Shape, Facet, Aspect Ratio, and Composition of the Nanorods. *Chem.—Eur. J.* **2005**, *11*, 910–916.
54. Haiss, W.; Thanh, N. T. K.; Aveyard, J.; Fernig, D. G. Determination of Size and Concentration of Gold Nanoparticles from UV-Vis Spectra. *Anal. Chem.* **2007**, *79*, 4215–4221.
55. Gole, A.; Murphy, C. J. Polyelectrolyte-Coated Gold Nanorods: Synthesis, Characterization and Immobilization. *Chem. Mater.* **2005**, *17*, 1325–1330.
56. Woehrle, G. M.; Hutchison, J. E.; Ozkar, S.; Finke, R. G. Analysis of Nanoparticle Transmission Electron Microscopy Data Using a Public Domain Image-Processing Program, Image J. *Turk. J. Chem.* **2006**, *30*, 1–13.
57. Bullen, C.; Zijlstra, P.; Bakker, E.; Gu, M.; Raston, C. Chemical Kinetics of Gold Nanorod Growth in Aqueous CTAB Solution. *Cryst. Growth Des.* **2011**, *11*, 3375–3380.
58. Li, Y.; Yamare, D. G.; Li, S.; Biswas, S.; Reddy, R. K.; Goettert, J. S.; Nandakumar, K.; Kumar, C. S. S. R. Geometric Optimization of Liquid-Liquid Slug Flow in a Flow-Focusing Millifluidic Device for Synthesis of Nanomaterials. *Chem. Eng. J.* **2013**, *217*, 447–459.
59. Larber, N.; Sarrazin, F.; Guillot, P.; Panizza, P.; Colin, A.; Pavagean, B.; Hany, C.; Maestro, P.; Marre, S.; Delclos, T.; *et al.* Some Recent Advances in the Design and Use of Miniaturized Droplet-Based Continuous Processes: Applications in Chemistry and High-Pressure Microflows. *Lab Chip* **2011**, *11*, 779–787.